

UC San Diego

UC San Diego Previously Published Works

Title

Robust design of microgrids using a hybrid minimum investment optimization

Permalink

<https://escholarship.org/uc/item/5nw0t4gc>

Authors

Pecenak, Zachary K

Stadler, Michael

Mathiesen, Patrick

et al.

Publication Date

2020-10-01

DOI

10.1016/j.apenergy.2020.115400

Peer reviewed

Robust Design of Microgrids Using a Hybrid Minimum Investment Optimization

Zachary K. Pecenak^{a,*}, Michael Stadler^{a,c,d}, Patrick Mathiesen^a, Kelsey Fahy^a, Jan Kleissl^b

^aXENDEE, 6540 Lusk Blvd., Suite C225 San Diego, CA 92121 USA

^bUC San Diego, 9500 Gilman Dr., San Diego, CA 92037

^cBioenergy and Sustainable Technologies, Austria

^dCenter for Energy and Innovative Technologies, Austria

Abstract

Recently, researchers have begun to study hybrid approaches to Microgrid techno-economic planning, where a reduced model optimizes the DER selection and sizing is combined with a full model that optimizes operation and dispatch. Though providing significant computation time savings, these hybrid models are susceptible to infeasibilities, when the size of the DER is insufficient to meet the energy balance in the full model during macrogrid outages. In this work, a novel hybrid optimization framework is introduced, specifically designed for resilience to macrogrid outages. The framework solves the same optimization problem twice, where the second solution using full data is informed by the first solution using representative data to size and select DER. This framework includes a novel constraint on the state of charge for storage devices, which allows the representation of multiple repeated days of grid outage, despite a single 24-hour profile being optimized in the representative model. Multiple approaches to the hybrid optimization are compared in terms of their computation time, optimality, and robustness against infeasibilities. Through a case study on three real Microgrid designs, we show that allowing optimizing the DER sizing in both stages of the hybrid design, dubbed minimum investment optimization (MIO), provides the greatest degree of optimality, guarantees robustness, and provides significant time savings over the benchmark optimization.

Keywords: Microgrid, economic planning, mixed-integer optimization, techno-economic optimization, DER-CAM, multi-energy systems, outages, islanded, XENDEE

Nomenclature

Indices

d	Day-type, $D = \{\text{Week, Weekend, Peak}\}$
e	End-use type, $E = \{\text{Electric, Thermal, Natural gas}\}$
f	Fuel type, $C = \{\text{Natural Gas, Diesel, Hydrogen}\}$
g	Discrete generation technologies (only available in discrete sizes), $G = \{\text{Internal Combustion Engine, Combined Heat and Power, Fuel cell}\}$
h	Hour, $H = \{1, 2, \dots, 24\}$
k	Continuous generation technologies (available in any size), $K = \{\text{Photovoltaic, Energy Storage, Absorption Chiller}\}$

m	Month, $M = \{1, 2, \dots, 12\}$
p	Tariff demand period, $P = \{\text{Non-coincident, Off-peak, Mid-peak, Peak}\}$
t	Technologies, $T = G \cup K$
Variables	
$CapCont_c$	The capacity of continuous generation technology c purchased
$FP_{m,d,h,f}$	Fuel purchased of type f at time-step m,d,h
$K_{m,d,h,e,t}$	Energy of type e consumed by technology t at time m,d,h
$L_{m,d,h,e}$	Energy demand of type e at time m,d,h
$PurchNum_g$	The number of units of discrete generators g purchased
$P_{m,d,h,e,t}$	Energy provided by technologies t for end use e at time-step m,d,h

*Corresponding author

$R_{m,d,h,t}$	Climate resource for technology type t at time-step m,d,h
$S_{m,d,h,e,t}$	Exports by technology t of type e at time m,d,h
$U_{m,d,h,e}$	Utility energy purchased for end use e at time-step m,d,h
Parameters	
ANN_t	Investment annuity rate of technology type t
$A_{m,d,h,e}$	$\in [0,1]$, binary availability of external energy providers
$CapGen_g$	The capacity of generator g
$Cdem_{e,p}$	Demand charge applied to period p for energy type e
$Ctax$	Carbon tax
EF_t	Emissions factor of technology t or the utility source
FOM_c	Annual Fixed O&M cost required for continuous generator c
FOM_g	Annual Fixed O&M cost required for discrete generator g
$FS_{m,f}$	Fixed service charge for month m and fuel f
$Icap_g$	Unit capital cost of discrete technology type g
$Ifix_c$	Fixed investment cost required for continuous technology of type c
$IntRate$	Interest rate on investment
$Ivar_c$	Variable investment cost required for continuous technology of type c
$ND_{m,d}$	Number of days of type d in month m
$PX_{m,d,h}$	Exchange price for electricity at time-step m,d,h
SC_m	Utility standby charge for month m
$Ufix_m$	Fixed utility charge for month m
VOM_t	Annual variable O&M cost required for technology of type t
$Vfuel_{m,d,h,f}$	Volumetric fuel price at time-step m,d,h for fuel type f
$Vutil_{m,d,h,e}$	Volumetric utility price at time-step m,d,h for energy type e
$lifetime_t$	Lifetime of technology type t

1. Introduction

Microgrids, often synonymous with multi-energy systems, are rapidly becoming a viable commercial strategy to provide resilience, cost savings, and decarbonization [1]. Microgrids are typically grid-tied systems which provide economic benefit, but are capable of islanding (disconnecting from the grid) and still supporting a significant portion of their demand for the duration of the disconnection, increasing resilience. In the extreme, some Microgrids (typically referred to as remote or off-grid Microgrids)

are never grid-tied and must support the entire system demand at each time instance [2].

However, before a Microgrid can be deployed, significant efforts go into planning to ensure stable and reliable operation and to quantify the return on investment [3]. These planning approaches must consider the expected power and energy demand, weather resources, regulations, cost of energy, DER operation and economics, and reinvestment strategy over the entire lifetime of the project, which can range from 10-50 years [4]. As the complexity of the planning model increases, for example by considering DER placement in the power distribution network [5], the time and cost required for the planning stage further increases.

Planning algorithms that can reduce the time between iteration and solution are extremely valuable [4, 6, 7]. Examples of this include linearizing the multiyear planning problem [4], clustering the input data, reducing the resolution of the solution [6], and reducing the size of the microgrid network [7]. The solve-time for a planning model is correlated with the size of the solution space it must examine. Therefore, an effective way to reduce solve-time is to minimize the size of the solution search space [8]. For a Microgrid planning tool, the solution space is the cardinal product of the considered DER types, DER sizes, DER placement locations, and DER dispatch possibilities at each time-step over the optimization horizon. Reducing even a few variables from the solution space can produce exponential savings in solve-time.

Different classes of planning algorithms attempt to reduce the run-time in different ways. A common technique used for Microgrid planning, the brute force simulator [9, 10], explicitly models each possible combination of DER over the planning window. For computational feasibility, typically only a small subset of DER sizes is considered. Further, these methods apply rule-based dispatch logic (not optimized), which makes the set of dispatch strategies for any set of DER extremely limited. Commercial examples of this model include HOMER [9] and RETSCREEN [10].

Linear optimization techniques (e.g. references [11–14]), on the other hand, quickly sift through the linear variables in the solution space to determine the

optimal solution. Commercial examples include the XENDEE economic model [3, 15] and NREL REOPT [16]. An advantage of these methods is the ability to provide an optimized dispatch strategy, that is unique for variations in DER size and type and superior to rule-based dispatch strategies.

Instead, for Microgrid planning optimization techniques, one well-accepted approach in the literature is the reduction of the input time-series data [6, 17–21]. Here, the annual time-series input data sources, typically at hourly (8760 time-steps) or 15 minute (35,040 time-steps) resolution, are compressed into a lower resolution or a set of days that are representative of the full time-series. These studies have shown that this approach is capable of producing consistent time savings of up to 98% including cases which typically took days being solved in a matter of minutes [21]. For a deeper literature survey on input reduction techniques, see references [6, 17, 21].

The time savings from input reduction come at the cost of two main outcomes compared to the benchmark full-scale (time-series) optimization (FSO): i) A reduction in optimality, which manifests in deviations in sizing and objective function; and ii) A lack of transparency of how the system behaves when subjected to the full time-series data (FSO).

Though item i) has been the focus of much research, item ii), the behavior of a system that was optimized using reduced time-series when subjected to the full time-series data has not been studied as extensively. References [6, 18, 19, 22] each solved two models consecutively in two stages (later defined as a hybrid optimization). In the “design stage” a simplified model solved the sizing, selection, and dispatch for representative days. In the “operation stage” a full-scale model with fixed types and sizes of DER, optimizes only the DER dispatch. Stadler et al. [21] showed that this two-stage approach brings the objective function closer to the FSO compared to the simplified design stage model alone. Since the 8760 h DER dispatch is significantly faster than 8760 h DER sizing and dispatch of the FSO, the two-stage model solve-times are only insignificantly larger than the solve-times for the design stage alone.

All of these methods were shown to be robust for grid-connected operation. When a utility connec-

tion acts as a central ‘marginal’ energy provider, the Microgrid demand can be guaranteed to be met for all time-steps, assuming no limit on import power. However, when operating in islanded mode, i.e. in the absence of a marginal energy carrier, the model must rely on load shedding to meet the energy balance, even if it is not desirable or costly.¹ Breaking the energy balance in this way, i.e. violating robustness, renders the solution and the time-savings useless.

Gabrielli et al. [22] showed there is a significant chance that the representative day model will recommend DER sizes which – while satisfying the representative (averaged) energy balance – will fail for at least one time-step in the full model. By studying thousands of scenarios, the authors showed that by increasing the representative demand profile uniformly the robustness can be enhanced, but optimality (closeness to FSO objective function) is compromised. While increasing the demand improves robustness at the cost of optimality, it does not guarantee it.

In this paper we introduce a new two-stage design approach, called minimum investment optimization, where the model is allowed to size the DERs in both stages to guarantee robustness, while maximizing optimality. This approach successfully designs Microgrids which operate robustly in islanded conditions. First – as in prior work – the design stage model estimate DER sizes. These sizes are then fed into a FSO model as a minimum size requirement, but the FSO model can invest in additional DERs to meet the energy balance or improve the objective function. The first stage significantly restricts the solution space, and therefore, the solve-time of the FSO.

Therefore, the contributions of this paper to the literature of Microgrid energy systems design using representative models are as follows:

- Introduction of a two-stage linear optimization method (MIO), which uses both reduced and

¹Another case when the energy balance may not be met in grid-connected operations is when there are power import constraints. This case will not be further discussed in the paper, but is also important in Microgrid applications.

full time-series to optimize DER sizing to reduce run-times over models only considering the full time-series. All prior representative or hybrid methods only sized DERs with the reduced timeseries. Such DER sizing cannot satisfy the microgrid energy balance during all timesteps in islanded conditions without load shedding. The MIO model guarantees robustness in islanded operation.

- The significance of the novel MIO method is that the guarantee of robustness comes at barely any increase in computational cost. In other words the novel MIO method resolves a long-standing seemingly irreconcilable issue between model reduction and the quality of the solution.
- A secondary contribution is a set of novel constraints on storage state of charge (SOC) that allows approximating storage dispatch (such as discharging) across multiple days in the reduced model. These constraints not only improve the optimality of the sizing using representative days, but also are beneficial in conjunction with the MIO method. Since the storage dispatch across multiple (apparent) days is closer to how storage operates in the full time series, the resulting representative solution will be closer to the optimal solution for the full time series and therefore decrease run times in the MIO.

The paper is organized as follows. Section 2 introduces the Mixed-Integer Linear Program (MILP) formulation which the hybrid approach is built on. Section 3 introduces the concept of robustness and the different robustness approaches studied in this paper. Section 4 tests the different approaches for three Microgrids subject to four single day outages, as well as a completely isolated off-grid scenario. The paper is concluded in section 5 and future work is discussed.

2. Overview of models and hybrid approach

2.1. Hybrid optimization (HO)

Here, a hybrid optimization is any method which uses a two-stage sizing method. In this paper we in-

troduce three novel hybrid optimization techniques, including one where both the downsampled representative optimization (RO) and the full scale optimization (FSO) sequentially select and size the DER investment (Fig. 1). In all approaches, the RO output provides bounds on investment in the FSO model. To differentiate between the FSO used as a benchmark for analysis, and the FSO used in the hybrid approach (which is constrained to a fixed or minimum investment), we call the latter the “time-series optimization” (TSO) in the rest of the work. We label the hybrid optimization as introduced in literature (with fixed DER capacities from RO applied to dispatch in TSO) as the benchmark hybrid optimization (BHO).

Both stages of our HO methods use the same problem formulation introduced in Section 2.2. RO and TSO are differentiated through a single input parameter that informs the optimizer over which set of days the optimization should occur (section 2.3). The TSO optimizes over the original 8760 h time-series profiles. In the RO, each time-series input is reduced to a set of representative day profiles (called “day-types”) as introduced in section 2.3.

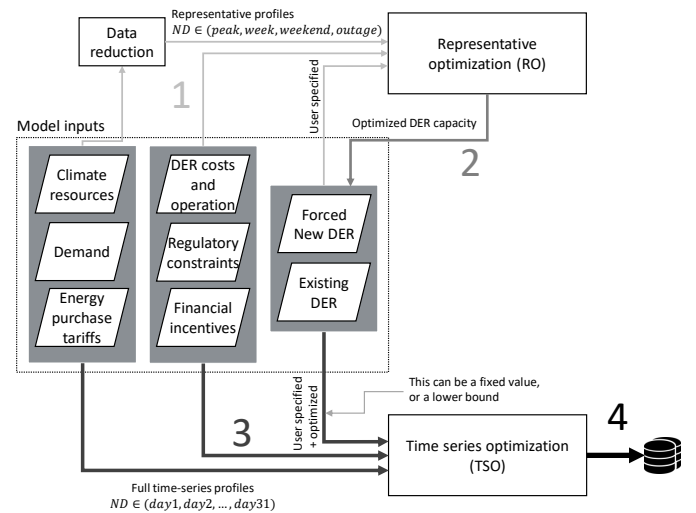


Figure 1: Flowchart of the four steps of the hybrid optimization. Step 1: Prepare and run RO which includes reduction of the input time-series data into representative profiles for normal and outage operation, and the modification of the number of days ND . Step 2: Update the user defined input data with the optimized DER investment selected in the RO. Step 3: TSO run with the full time-series data, and the DER investment as either a fixed value (see BHO, MDM, WWD methods), or a lower bound (MIO method). Step 4: Record and report the economics, dispatch, and investment from the TSO model.

2.2. Optimization formulation

The studied optimization problem is the professional version of the XENDEE platform [3, 4, 15],

which is formulated based on the LBNL DER-CAM model [5, 23, 24]. The XENDEE platform provides a user-friendly interface to define system parameters, input data sets, and set model constraints for the optimization model described here.

The objective function minimizes the total cost required to operate the Microgrid, by optimally sizing multiple energy sources considering economic and physical equations and the operation for each time-step in the optimization window. The time-steps are characterized by time-series data over a full year of data at hourly or finer resolution, such as weather-dependent resource availability, demand, and real time utility price. The time-steps of the optimization are represented using indices m, d, h for the month, day, and hour of the optimization, respectively. The model can either consider a full year (a FSO), or a set of representative downsampled days (a RO, see section 2.3). The portion of the objective function, which focuses on minimizing cost (emissions are not optimized in this paper), is:

$$\min C : C_{\text{tariff}} + C_{\text{fuel}} + C_{\text{DER}} + C_{\text{CO}_2} - r_{\text{sales}} \quad (1)$$

subject to

$$\begin{aligned} \text{Energy Balance} : L_{m,d,h,e} + \sum_{t \in T} (S_{m,d,h,t,e} + K_{m,d,h,t,e}) \\ = \sum_{t \in T} P_{m,d,h,t,e} + U_{m,d,h,e} \end{aligned} \quad (2)$$

where

$$\begin{aligned} C_{\text{tariff}} : \sum_{m \in M} U_{\text{fix}_m} \\ + \sum_{m \in M, d \in D, h \in H, e \in E} V_{\text{util}_{m,d,h,e}} \cdot U_{m,d,h,e} \cdot \text{ND}_{m,d} \\ + \sum_{p \in P, e \in E} \max(U_{e,p}) \cdot C_{\text{dem}_{e,p}} \\ + \sum_{m \in M} \left[\sum_{g \in G} \text{PurchNum}_g \cdot \text{CapGen}_g \right. \\ \left. + \sum_{g \in G} \text{CapCont}_g \right] \cdot \text{SC}_m \end{aligned} \quad (3)$$

$$\begin{aligned} C_{\text{fuel}} : \sum_{m \in M, f \in F} \text{FS}_{m,f} \\ + \sum_{m \in M, d \in D, h \in H, f \in F} \text{FP}_{m,d,h,f} \cdot \text{ND}_{m,d} \cdot V_{\text{fuel}_{m,d,h,f}} \end{aligned} \quad (4)$$

$$\begin{aligned} C_{\text{DER}} : \sum_{g \in G} \text{PurchNum}_g \cdot \text{CapGen}_g \cdot \text{FOM}_g \\ + \sum_{k \in K} \text{CapCont}_k \cdot \text{FOM}_k \\ + \sum_{m \in M, d \in D, h \in H, t \in T} \sum_{e \in E} P_{m,d,h,t,e} \cdot \text{ND}_{m,d} \cdot V_{\text{OM}_t} \\ + \sum_g \text{PurchNum}_g \cdot \text{Icap}_g \cdot \text{ANN}_g \\ + \sum_k \left[\text{PurB}_k \cdot \text{Ifix}_k \right. \\ \left. + \text{CapCont}_k \cdot \text{Ivar}_k \right] \cdot \text{ANN}_k \end{aligned} \quad (5)$$

$$C_{\text{CO}_2} : \sum_{m \in M, d \in D, h \in H} \left[\sum_{t \in T, e \in E} P_{m,d,h,t,e} \cdot \text{EF}_t \right] \cdot \text{ND}_{m,d} \cdot \text{Ctax} \quad (6)$$

$$r_{\text{sales}} : \sum_{m \in M, d \in D, h \in H} \sum_{t \in T} S_{m,d,h,t,\text{elec}} \cdot \text{PX}_{m,d,h} \quad (7)$$

$$\text{ANN}_t : \frac{\text{IntRate}}{1 - \frac{1}{(1 + \text{IntRate})^{\text{ifetime}_t}}} \quad (8)$$

$$\text{Purchase limit} : U_{m,d,h,e} \leq \bar{U}_{m,d,h,e} * A_{m,d,h,e} \quad (9)$$

Here, the five terms being minimized ($C_{\text{tariff}}, C_{\text{fuel}}, C_{\text{DER}}, C_{\text{CO}_2}, r_{\text{sales}}$) in the objective function (eq. (1)) are described in terms of decision variables in eq. (3) - (7). These terms indicate how the optimizer minimizes costs by balancing the costs of purchasing electricity (eq. (3)) and fuel (eq. (4)) with purchasing and operating DER technologies (eq. (5)). An amortization rate (eq. (8)) transforms the DER upfront purchase cost into an annual equivalent cost, to allow for the comparison with operational costs. Equation (9) forces purchases to zero during outage hours. Finally, the energy balance is enforced for each time-step (eq. (2)) of the optimization. The full algorithm is described in more detail in earlier works, see [4, 5, 25].

2.3. RO versus TSO modeling

The flexibility to handle either a continuous yearly time-series, or a smaller subset of time-steps

in the problem formulation introduced in Section 2.2 is due to the use of indices explicitly describing the month m , day d , and hour h of the optimization window. For both RO and TSO models we assume a 12 month (m) and 24-hour (h) set of steps, but the set of days (d) varies depending on the application of the model as codified by the term $ND_{m,d}$.

Specifically, the matrix relates the number of times a certain day (d) will occur in a month (m). For the FSO, we define d as a set of 31 days ($d \in \{\text{day1, day2, ..., day31}\}$) and $ND_{m,d}$ is a binary matrix that ensures that only calendar days are optimized: entries for days d in month m which occur in that month (i.e. February 1-28) are equal to one, while days which do not occur (i.e. February 29, June 31, etc.) have an entry of zero.

Time-steps can also indicate representative day-types in each month ($m \in \{1, 2, \dots, 12\}$), with the same temporal resolution (one hour in our example). Specifically, we employ three peak-preserving representative days, a typical peak, week, and weekend day profile as introduced in reference [17]. Distinct week and weekend profiles are needed to capture variations in time-of-use energy rates, while the peak day captures the monthly demand charges. As in [17], the week and weekend profiles are created by binning all days into two groups, based on if they occur on a weekday (Mon-Fri) or a weekend (Sat-Sun) and taking the average of the load across each hour in each bin. The peak day is an artificial day, which is created by searching across all the days in a month (one bin), and selecting the peak demand at each hour. This method ensures that demand peaks are preserved in the down-scaled representative days. All other time-series inputs, such as ambient temperature, solar irradiance, and wind power potential, are considered uncorrelated to the load profile. Therefore, for each of the daytypes (i.e. week, weekend, peak), the same monthly-averaged 24-hour profile (of irradiance, wind performance, etc.) is used. This approach is elaborated and justified in [17, 21].

For the representative data sets, the day-types set d includes the three day-types introduced above ($d \in \{\text{peak, week, weekend}\}$). Here, $ND_{m,d}$ is no longer binary, and is used to scale up the occurrence of a day-type back to a month of operation, thus $\sum_d ND_{m,d}$ must equal the number of calendar days in a month.

We consider only 1 peak day for each month (thus $ND_{m,\text{peak}} = 1$), which is assumed to occur on a weekday. For example, for January 2020, $ND_{m,\text{week}} = 22$ and $ND_{m,\text{weekend}} = 8$. Thus, it is assumed that the behavior of a weekday happens 22 times in the month.

2.4. Outage modeling in RO

To allow for power outages, generator maintenance down-time, or demand response events in the RO, additional day-types can be introduced to the set d and the $ND_{m,d}$ can be modified. Since modeling outages is a central focus of Microgrid research and this work, we introduce a fourth day-type, the outage day ($d \in \{\text{peak, week, weekend, outage}\}$). This day is characterized by a period of disconnection from the utility, where the Microgrid must meet the demand profile specified, or shed the demand at a specified cost to satisfy the energy balance of the optimization. Here the outage can range from 1 hour to 24 hours on the outage day. If multiple day outages are desired, $ND_{m,\text{outage}}$ can be set to a non-binary value (while adjusting the balance of the total number of days). For the outage day-type a second profile is introduced for other time-series variables such as ambient temperature, solar irradiance, and wind power potential (section 3).

2.5. State of charge constraints

An important constraint is applied to the 'state-of-charge' (SOC) of all storage technologies that are considered in the model including electrical batteries, flow batteries, thermal/cold storage, or hydrogen tanks. In the case study of section 4, we focus exclusively on Li-ion storage devices, as that is the most common use case in the XENDEE platform. For the FSO, the SOC is constrained based on physical limits (min and max), the SOC in the previous time-steps, and the maximum hourly charge/discharge rates. The optimization is formulated such that the SOC at any time-step is equal to the previous time-step less the energy consumed or discharged:

$$SOC_{m,d,h,e} = SOC_{m((-1), d((-1), h(-1), e} - \tilde{K}_{m,d,h,e,\text{storage}}, \quad (10)$$

where a double dash indicates a circular lag, meaning that the optimization treats the last and first elements of a set as consecutive elements (i.e. look at

hour 24, if currently hour 1). The parentheses indicate that that the circular lag is only considered if the time-step is the first of the day or the month e.g. the SOC at hour 1 on January 1 is linked to the SOC at hour 24 on December 31. \tilde{K} indicates the fractional energy discharged $\tilde{K}_{m,d,h,e,storage} = K_{m,d,h,e,storage}/Capacity_{storage}$

For the RO, to ensure consistent storage operation across each day-type, a circular constraint on the storage SOC is applied across each day-type, instead of the full year:

$$SOC_{m,d,h,e} = SOC_{m,d,h-1,e} - K_{m,d,h,e,storage} \quad (11)$$

Note the removal of the connection to other day-types and months. The SOC at hour 24 is linked to the SOC at hour 1, creating a circle. This constraint ensures that the specified day-type is able to be repeated consistently as specified by $ND_{m,d}$ (i.e. 22 times in January).

For an outage day, the circular SOC constraint can be troublesome for storage-only, or solar PV and storage projects which are heavily space constrained. Since there is no connection to the utility, it might not be possible to meet the load and recharge the battery to meet the SOC constraint in eq. (11). However, continuous storage discharge during an outage event without recharging is a common use-case, and is a likely strategy employed by the FSO (and TSO).

To overcome this limitation, we introduce a new constraint, which allows the storage to discharge such that the circular SOC constraint is no longer enforced (i.e. SOC at hour 1 is not necessarily within one charge cycle of hour 24). The following three constraints represent this formulation:

$$SOC_{m,d,1,e} \leq \overline{SOC} \quad (12)$$

$$SOC_{m,d,h,e} = SOC_{m,d,h-1,e} - K_{m,d,h,e,storage} \quad (13)$$

$$SOC_{m,d,24,e} \geq \overline{SOC} \times \frac{(ND_{m,outage} - 1)}{ND_{m,outage}} \quad (14)$$

Here \overline{SOC} indicates the upper limit on SOC. Equation (14) specifically indicates that the storage must reserve enough energy at hour 24 (i.e. the end of the day) such that the discharge profile can be repeated for the number of outage days being planned (i.e.

$ND_{m,outage}$). As an example, a storage system providing energy for a 5 day outage would reserve at least 4/5 of its total energy (80%) at the end of the outage day, such that it could continue to discharge 20% of its total energy during each of the next four days. Together, these three equations allow the storage to discharge from the beginning of the outage day though the end, as long as the storage can continue discharging for the number of outage days ($ND_{m,outage}$). This approach is illustrated for a single 24-hour outage in figure 2.

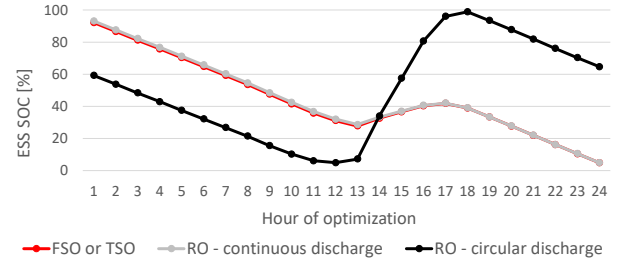


Figure 2: A comparison of the three SOC approaches (equations (10)-(14)) when applied in the model to an optimization with a single 24-hour outage

3. Modeling robustness and adequacy indicators

3.1. Adequacy indicators

Following [17–19, 21], the indicators to measure the performance of the method are optimality and time savings. Time savings TS is simply defined as the difference between the wall clock run-time for the benchmark FSO, and that of the entire HO, normalized to give the fractional savings

$$TS = \frac{T_{FSO} - T_{HO}}{T_{FSO}}. \quad (15)$$

Optimality Opt is defined as the difference between the objective functions J measuring the annual cost of the HO and benchmark FSO, and is here also defined in terms of a fractional difference

$$Opt = 1 - \frac{J_{FSO} - J_{HO}}{J_{FSO}}. \quad (16)$$

Robustness, defined as the ability for a system to meet the energy demand at each time-step, is another important adequacy measure for both grid-connected and islanded Microgrids. Reference [22] introduced a robustness metric which captures unmet thermal

demand on an annual basis in a reduced model. Here, we introduce a similar metric and expand the definition to electricity. We do not allow load curtailment, though XENDEE can optimize curtailment at up to 3 levels of the total demand in each time-step. Instead, a new variable is introduced to the energy balance, $ME_{m,d,h,e}$, which measures the marginal energy required to meet the energy balance at any time-step.

$$\text{Energy Balance}^* : L_{m,d,h,e} + \sum_{t \in T} (S_{m,d,h,t,e} + K_{m,d,h,t,e}) \quad (17)$$

$$= \sum_{t \in T} P_{m,d,h,t,e} + U_{m,d,h,e} + ME_{m,d,h,e} \quad (18)$$

To prevent $ME_{m,d,h,e}$ from taking a non-zero value, in the objective function it is heavily penalized through multiplication by 10^6 , similar to the concept of a slack variable. We define the robustness as the summation of the absolute value of $ME_{m,d,h,e}$ normalized by the load as

$$R = 1 - \frac{\sum_{m,d,h,e} ME_{m,d,h,e}}{\sum_{m,d,h,e} L_{m,d,o,e}} \quad \forall m, d, h \text{ in outage} \quad (19)$$

Note that DER downtime/failure is ignored in this analysis, despite the potential for significant impact on the robustness measure. For a discussion on how XENDEE handles DER contingencies, see reference [26].

3.2. Approaches to improve robustness

3.2.1. Shortcomings of the existing hybrid optimization approach

The basic two-stage BHO approach discussed in the literature assumes that the sizes selected in the RO are robust, i.e. produce feasible results by satisfying the energy balance in the TSO. This assumption is challenged, however, under scenarios in which there is no grid connection to provide the marginal energy needed to satisfy the energy balance. During outages, the TSO will require all demand in the outage window to be met through the purchased DER, considering the available climate resource during that window and the energy stored at outage start. However, the RO optimization cannot guarantee all TSO demand to be met because of the following reasons:

1. Outages greater than 24 hours cannot be represented in the RO, since the RO generally does not represent subsequent days.
2. Since TSO is continuous in time, conditions on the surrounding days can impact dispatch. RO outages, on the other hand, are modeled as isolated events.
3. The climate resource and demand profile on the RO outage day can differ from TSO.

Table 1 shows an overview of the HO approaches to improve robustness and they are described in more detail in turn.

3.2.2. Worst window day (WWD)

One challenge outlined above is the choice of climate resource and demand profiles during the RO outage day to accurately size the DER. WWD is designed to select the demand and solar profiles used in the RO of the hybrid approach, which are the most difficult from an energy balance perspective. The underlying hypothesis is that if the DERs can meet the energy demand on this “worst” day, they can do the same for all other days. However, since the “worst” day depends on DER sizing (e.g. if more solar power is installed, the worst day would be a day with the worst solar irradiance) its selection is ambiguous and cannot be known during the first stage of the optimization. Even if no DERs are considered, it is a priori unclear if the worst day is the day with the largest demand peak or the day with the largest total energy consumption.

Since the goal of this paper is to prevent energy imbalances, WWD uses artificial demand and climate resource profiles which constitute the worst possible combination of demand and climate resource over each month. These are not profiles from any particular day within the window, rather they are representative hourly profiles constructed by finding the maximum demand and the minimum climate resource in each hour. Figure 3 gives an example of such profiles for demand and solar PV resource. Note that the same approach is used to construct the representative peak demand day discussed in section 2.3, but this approach is now extended to the climate resources.

WWD represents an extreme of the two-stage BHO approach in the literature, as the artificial pro-

files represent the absolute worst case that can be modeled using the given data. This is descriptive, as it demonstrates the upper limit of the robustness provided by traditional BHO approaches. WWD may result in over-sizing if the worst case is much worse than situations that are actually encountered during the 8760 hours. The run-time for WWD should be on par with the BHO in literature, as WWD requires only a single RO run and only dispatch is optimized in the TSO.

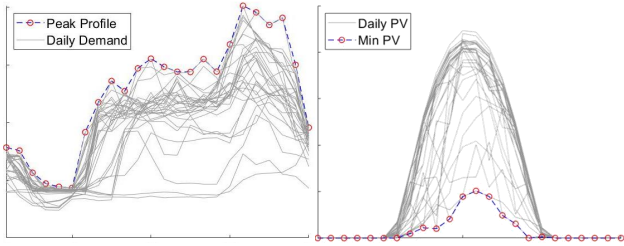


Figure 3: Construction of the artificial worst day profile: (left) The demand “peak” profile is created by finding the maximum demand in each hour. (right) The solar PV resource “min” profile is constructed by finding the minimum value in each hour.

3.2.3. Marginal demand modification (MDM)

MDM is characterized by a repeated trial-and-error approach, where the HO (with fixed investment determined in RO) is used twice, sequentially. The lack of robustness in the first stage is resolved in the second stage by increasing the RO outage demand profile artificially to include additional demand that was not met during the TSO in stage 1 (Fig. 4).

In the first analysis, the RO is optimized using a representative profile. The fixed DER investment from the stage 1 RO is input to the TSO. From the TSO output a new supplemental hourly demand profile is created as the maximum of the marginal energy unmet in each hour of a month $\max_h(\text{ME}_{m,d,h,e})$ (red bars in Fig. 4). The supplemental demand profile is added to the original RO outage demand profile, and is used in the RO of the second analysis.

Given that the unmet demand is exactly added to the RO representative demand, the result of the stage 2 optimization is hypothesized to guarantee robustness yet still prevent oversizing and therefore ensure good optimality. However, the robustness of MDM may also be compromised by not addressing issues 1 and 2 in the list provided in section 3.2.1. The

run-time should be generally predictable, and take around twice as long as the WWD analysis.

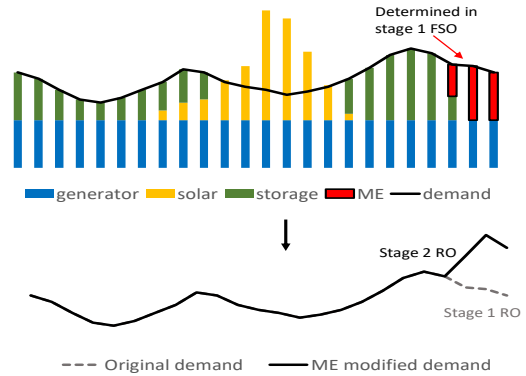


Figure 4: Marginal Demand Modification: Missing Energy (ME) in the stage 1 TSO (red in the upper graph) is added to the demand profile (lower graph) before the second loop of the RO.

3.2.4. Minimum investment optimization (MIO)

MIO differs from WWD and MDM in that the TSO is allowed to modify the RO sizing, addressing all issues in the list provided in the previous section. MIO has not been previously discussed in the literature, to the knowledge of the authors. In MIO, the optimal investments / sizing determined in the RO are considered as a lower bound. This approach guarantees robustness, since the TSO can invest in additional DER needed to meet the energy balance. Yet compared to a FSO, the RO solution restricts the solution space of the TSO, thus reducing run-time. While the solution space could be further restricted by applying a sensible upper bound on the possible investment and/or upper or lower bounds on certain DERs, we do not consider upper bounds in this paper.

MIO guarantees robustness of the hybrid optimization, but does not guarantee a run-time reduction. Rather, it is expected that run-time savings would increase as the accuracy of the RO solution increases, since the greatest reduction in solution space is gained. MIO is also expected to perform near optimality; the only scenario where optimality can be worse than the FSO is if the DER size in the RO solution is larger than the size in the FSO solution; then the solution space in the TSO would be too restricted and the TSO could not downsize the DER to its optimal size.

Table 1: Comparison of the robustness models.

Model	Principal of Operation	HO Strategy	Data modeled
WWD	Size for worst case scenarios for load and solar generation	RO (sizing) and TSO (dispatch)	Artificial profiles of min. solar resource and max. demand
MDM	Trial & error: Unmet demand (ME) in TSO is added to load	(1) RO (sizing) and TSO (dispatch and determine ME) (2) RO (sizing considering ME) and TSO (dispatch)	Rep. days and Act. days
MIO	Minimum DER size bounds reduce solution search space	RO (sizing) and TSO (sizing & dispatch) with lower bounds from RO.	Rep. days and Act. days

Table 2: Microgrids studied. Tariff abbreviations are as follows: FER - Flat energy rate; TOUER - Time-of-use energy rate; NCDC - Non-coincident demand charge; PDC - Peak demand charge; MPDC - Mid-peak demand charge. DER abbreviations are as follows: PV - solar photovoltaic arrays; ESS - electrical energy storage systems; ICE - Internal Combustion Engines.

Name	Type	Location	DER modeled	Tariff characteristics	Annual energy consumption [MWh]	Peak annual consumption [kW]
MG1	University	California	PV, ESS, ICE	TOUER, NCDC, PDC	825	204
MG2	Public	Connecticut	PV, ESS, ICE	TOUER, NCDC	1,639	374
MG3	Pharma.	Puerto Rico	PV, ESS	FER, NCDC, PDC, MPDC	22,642	3,963

4. Case study

4.1. Microgrids

The HO solutions introduced in the previous section are tested with a focus on outage scenarios. Three real Microgrids are described in table 2 and were introduced in reference [21]. The set of Microgrids are meant to represent multiple demand profiles, geographies, and tariff structures. For simplicity and clarity, only electrical loads are considered. The analysis neglects limitations in the Microgrid power infrastructure such as line ratings or nodal voltage violations. The only renewable resource is assumed to be solar PV, thus only demand and solar resource profiles are considered.

Table 3: The four outage days selected for each Microgrid as determined by the benchmark optimization. Outage days 1 and 2 (O1,O2) are the days that cause the two largest objective functions. Outage 3 (O3) is the median objective function, while outage 4 (O4) is the lowest objective function. The no outage objective function value is provided for reference. The presented objective function is the non-integer solution, and thus provides a lower bound on the solution.

		MG1	MG2	MG3
Outage 1 (O1)	Date	Feb. 15	Aug. 12	Aug. 16
	J [k\$]	\$137.6	\$335.8	\$6,710.6
Outage 2 (O2)	Date	Feb. 2	Aug. 3	Sep. 14
	J [k\$]	\$137.1	\$326.4	\$6,708.2
Outage 3 (O3)	Date	Sep. 19	Jun. 25	Nov. 4
	J [k\$]	\$132.6	\$316.2	\$5,706.4
Outage 4 (O4)	Date	Jul. 1	Dec. 20	Feb. 25
	J [k\$]	\$132.4	\$315.9	\$4,431.0
No outage	J [k\$]	\$132.4	\$315.9	\$4,431.0

4.2. Outage modeling

A set of 24-hour outages starting at midnight are modeled to occur on four different days of the year, which are described in table 3 for each of the three Microgrids, producing $4 \times 3 = 12$ total outage scenarios. The objective function cost serves as a proxy of how challenging it is to provide all energy on the outage day. Objective function cost increases come from over-sizing DERs past the no-outage optimum to meet the required demand. The four outage days are the two days with the largest (O1, O2), the median (O3), and the day with the lowest objective function cost (O4). Note, as (O4) is the easiest outage to meet, for all three microgrids its objective function is identical to that of the cost optimal non-outage solution, indicating no additional investments are required. These choices allow analyzing the sensitivity of the robustness of each technique to the severity of outage day.

The outage days objective functions are obtained from benchmark FSO solutions in which a 24-hour outage is iteratively assigned to each day of the year, i.e 365 runs were conducted. To save on run-time, the relaxed non-integer solution was used, since only the objective function was needed.

In a separate case study, the Microgrids are assumed to be islanded for the entire year. This case is the most extreme challenge for robustness. For always islanded conditions, the selection of outage day profiles in the RO becomes more obscure, since only

a single outage profile is used to size DER to meet the load throughout the entire year. We examine the impact of the same set of day-types as above (four outage days in addition to the representative days) to represent the isolated Microgrid.

In both the single day outage and the off-grid study, we examine the impact of different RO demand/solar profiles in MIO and MDM. For each outage day, we consider: (i) the demand/solar profiles of that actual day (referred to as “Act. day” in the figures; E.g. an outage on Feb. 15 will use the solar and demand profiles from Feb. 15 in the RO); (ii) the monthly average solar and the day-types ‘peak’ load day of the month (see Section 2.3). In the figures, “Rep. day” denotes when the representative profiles are used.

4.3. Results

All three robustness approaches improved on the standard BHO (Fig. 5). Yet MIO is the only approach to guarantee 100% robustness for both the single day outage and the off-grid scenario. The WWD approach prevents infeasibilities for a single day outage, but infeasibilities exist for the off-grid scenario. For all methods, other than MIO, the off-grid scenario lead to a larger likelihood of infeasibilities. For both the BHO and MDM approaches, real day profiles improve the robustness over averaged profiles.

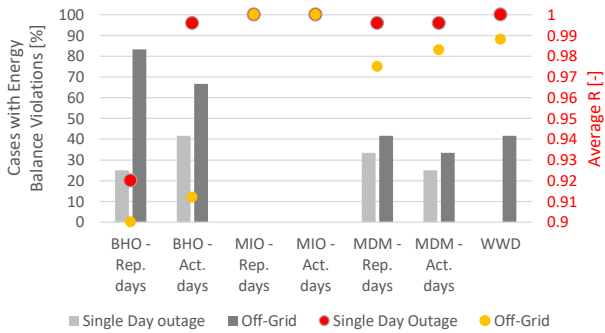


Figure 5: Two-axis plot showing (left, bars) the percentage of scenarios (out of 12) which did not meet the energy balance of the 12 outage scenarios and (right, dots) the average robustness for the 12 scenarios.

Fig. 6 shows run-times on a remote windows server with AMD Ryzen 5 3600 Hexa-Core with 64 GB DDR4 Ram and 2x512 GB NVMe SSD. All methods produce significant run-time savings over the FSO benchmark for MG1 and MG2, while only some methods produce run-time savings for

MG3. MG1 and MG2 have significantly longer run-times due to the consideration of investment in ICEs, which have a discrete decision variable. Such decision variables are notoriously hard for linear programming methods to solve. The MDM approach, while still providing significant run-time savings for MG1 and MG2 compared to the benchmark FSO, produced the longest run-times of all robustness methods, and actually caused run-time increases over the benchmark FSO for MG3. The long MDM run-times are due to the two consecutive HO runs.

Note, even though it optimizes in both the RO and the TSO stages, MIO has run-times on the order of the BHO and WWD methods which consider fixed investment in the TSO stage. The trends by outage day are inconsistent; for MG3 the run-times are independent of outage day, while for MG1 and MG2 the worst (O1) and easiest (O4) cause the longest run-times, respectively. A summary of the optimal-

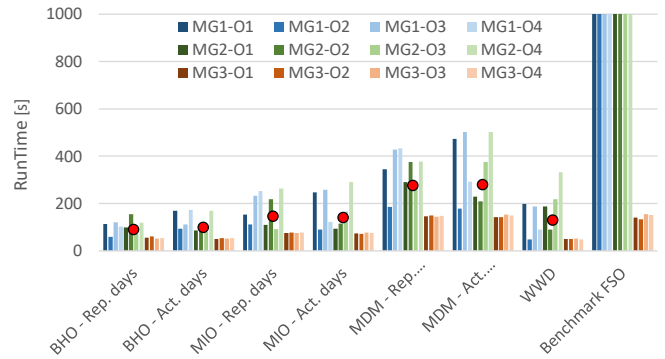


Figure 6: Absolute run-time for each method for the three Microgrid and four outage day scenarios. Off-grid model run-times are similar and follow the same trend, and thus are not shown. Microgrids are organized in color groups (blue-MG1, green-MG2, red-MG3) with the colors lightening as the severity of the outage day lessens (O1-O4). The mean of each method across all 12 scenarios is given by the red dot. The benchmark FSO for MG1 and MG2 extend beyond the y-axis limits is above the upper bound for the y-axis.

ity, robustness, and run-time savings is presented in Fig. 7. The (literature based) BHO methods produce the worst results of all methods. The MDM methods produces neither optimal solutions, or significant run-time savings. The WWD produces significant time savings, but cannot guarantee optimality or robustness. Typically the loss in optimality is found for “easier” outages (O3, O4; see table 3), where the WWD method oversized the DER. The MIO method tends to cluster to the upper right of the plot, indicating a high degree of optimality, robustness, and time savings. The MIO data points with smaller time

savings (40%) are attributed to MG3, which solves very quickly for the benchmark FSO, providing limited opportunities for additional time savings by restricting the solution search space (see Fig. 6). Sev-

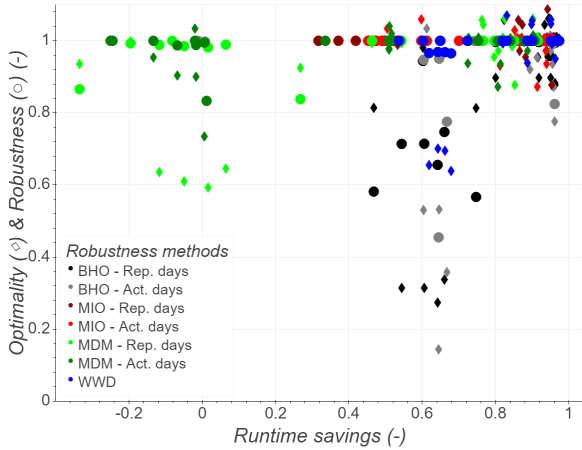


Figure 7: Summary plot showing the optimality, robustness, and run-time savings for the different methods over all outage scenarios and the offgrid analysis. The abscissa is run-time savings, while the ordinate quantifies both optimality (circles) and robustness (diamonds) as normalized values. Approaches that cluster to the top and right are desirable.

eral observations can be drawn from the DER sizing and objective function data in table 4. For the smallest Microgrid MG1, despite significant differences in DER investment between WWD and the benchmark, the objective function error is smallest. For the grid-connected cases for MG2, WWD over-sizes ICE, leading to an increased objective function. For MG3 off-grid, all cases except MIO result in energy balance violations, while MIO replicates the exact result of the 140 second benchmark FSO in only 75 seconds.

Regarding the sizing of individual DER types, the results are inconclusive. WWD tends to favor more ICE (MG1 and MG2) and less ESS and PV. This makes sense as the worst solar resource underestimates the PV contribution to meeting the load. However, despite the disparate sizing, the objective function for WWD is within 6% of the other approaches for MG1 and MG2. The sizing of the other methods is consistent across the 24-hour outages, but diverges for the off-grid scenarios for MG2 and MG3. For those scenarios MIO represents the sizing that is closest to the benchmark FSO again underscoring its superiority.

Table 5 breaks the results for MG3 into the different stages of the optimization for the BHO and MIO

models, as well as the benchmark FSO for comparative purposes. For all cases, it is clear the RO is an extremely fast option compared to the higher resolution models. However, it is observed that considering the TSO can improve the objective function and the DER sizes (i.e. closer to the benchmark). The runtime difference between RO and the benchmark is considerable in all cases, typically adding at least 2 minutes (the runtime difference is even more extreme for MG1 and MG2 which are not shown in this table). In contrast, both BHO and MIO provide solutions which take less than half the time required to run the full FSO. However, in all cases MIO provides a solution which is closer to the benchmark. Also, consistent with other results, using the actual daily profiles provides a solution much closer to the optimal and saves runtimes.

4.4. Discussion

From the results we can draw several conclusions about the robustness of the approaches. First, the standard two-stage HO, where DER sizes that are determined in the RO are fixed in the TSO, results in significant run-time savings, but violates the energy balance for off-grid cases, regardless of input data considered. The WWD scenario, which can be viewed as an extreme HO case, provided sufficient robustness for the 24 hour outages, but did not for the off-grid scenario. Thus, these two-stage methods do not guarantee robustness for Microgrids which have to sustain islanded conditions, which motivates the need for methods which guarantee robustness.

Second, when considering real data, the MDM performed well for the single day outages, producing negligible robustness violations (most likely due to numerical issues). A small increase in ME could resolve this problem with negligible impact on optimality. However, the MDM method performed poorly for the offgrid scenarios and the single-day outage considering the representative profiles. This is due to a lack of correlation of the solar generation between the RO profile and the TSO time-series. In addition to adding ME to the demand, the solar profile used in the sizing need to be corrected to be representative of periods where the RO and the TSO solar profiles diverge. In general, the robustness results show that the stochasticity of renewable resource

Table 4: A subset of the case study data for the O1 24-hour and the off-grid cases for all Microgrids and robustness approaches with the actual day data. The O1 case is representative of the worst case planning model, which is the most typical use case to consider. For each case the objective function J , the selected capacities of PV, ESS, and ICE, and the marginal energy (ME) are given. Solutions with objective function marked *infeas* are results that were infeasible and did not meet all of the demand (see ME).

Name	Model	24-hour outage					Off-grid				
		J [\$k]	PV [kW]	ESS [kWh]	ICE [kW]	ME [MWh]	J [\$k]	PV [kW]	ESS [kWh]	ICE [kW]	ME [MWh]
MG1	BHO	140.9	313	540	100	0	141.0	313	540	100	0
	MIO	140.9	312	540	100	0	141.0	312	540	100	0
	MDM	140.9	312	540	100	0	141.0	312	540	100	0
	WWD	139.7	174	0	200	0	140.6	174	0	200	0
	Benchmark	139.7	272	541	100	0	139.7	277	541	100	0
MG2	BHO	336.7	715	838	300	0	<i>infeas</i>	715	838	200	2.92
	MIO	336.7	715	838	300	0	336.7	715	838	300	0
	MDM	336.7	715	838	300	0	336.7	715	838	300	0
	WWD	357.0	715	780	400	0	357.0	715	780	400	0
	Benchmark	336.7	715	1160	200	0	336.7	715	838	300	0
MG3	BHO	<i>infeas</i>	17148	55573	0	0.05	<i>infeas</i>	17148	55573	0	1127.64
	MIO	6713.3	17148	55628	0	0	11232.9	42655	77007	0	0
	MDM	6713.7	17157	55616	0	0	<i>infeas</i>	18143	122669	0	257.84
	WWD	8190.1	17135	87572	0	0	<i>infeas</i>	17135	87572	0	702.21
	Benchmark	6710.6	16774	56192	0	0	11232.9	42655	77007	0	0

data combined with load data is very difficult if not impossible to capture with “ad-hoc” approaches such as WWD and MDM. While both WWD and MDM significantly improve the robustness compared to the BHO in the literature, producing a non-robust or non-optimal result is not acceptable for runtime savings, making MIO the only viable approach for a commercial method.

Third, the MIO method is the preferred method as it guarantees robustness, produces high optimality, and provides significant run-time savings for all cases. However, for MIO if the RO input data does not represent the outage well, the RO might improperly size DER. For example, if the RO profile over-sizes DER, the objective function of the TSO will be much higher than the benchmark FSO violating optimality. Alternatively, if the RO undersizes DER, the solution space is not sufficiently restricted, and run-time savings would suffer (not observed in this work). To overcome this, it is recommended to carefully select the RO input data, such as using the actual data from the outage window. Further, imposing upper bounds on all DER, but especially ICE units, which have the most significant impact on run-time (consider MG1 and MG2 versus MG3) would reduce run-times.

Finally, DER selection and size was not a reliable indicator of optimality. For several cases, disparate DER configurations (type and size of DERs) produced nearly identical objective functions and ME. None of the methods consistently produced identical

DER configurations to the benchmark. The exception was MIO in the off-grid scenarios, where the RO method would undersize DERs, and the TSO could increase DER sizes to match the benchmark FSO.

5. Conclusion

In this work, we introduce a techno-economic hybrid optimization framework, specifically designed to optimize the Microgrid design considering resilience to grid outages. All prior representative or hybrid optimization methods (HO) in the literature only sized DERs with the reduced timeseries. We show that such DER sizing is not robust, i.e. the DERs cannot satisfy the microgrid energy balance during all timesteps in islanded conditions without load shedding. The MIO model, on the other hand, guarantees robustness in islanded operation. The significance of the novel MIO method is that the guarantee of robustness comes at barely any increase in computational cost. In other words, the novel MIO method resolves a long-standing seemingly irreconcilable issue between model reduction and the quality of the solution.

The MIO employs a two step process, where it solves the same optimization problem twice, using different time resolutions. First a representative model, which uses reduced time-series, optimizes DER sizes, which are used to inform a full scale model in the second step. The second step takes advantage of the reduction in solution space provided

Table 5: The difference in decision made for each stage of the models, for both the grid-connected outage, and the off-grid system considering averaged and real profiles for solar and load. The RO model is considered the baseline in the table, and all numbers indicate deviations from that solution made in the TSO. The comparison is made against the BHO model (the typical approach in literature), which assumes fixed assets size in the RO and only optimizes dispatch in the TSO, the MIO method (a novelty of this work) which optimizes in both the RO and TSO stage, and the benchmark FSO which is considered to be the target for results in this paper. The RO is given in absolute values, while the other three models show only the incremental change from the RO optimization. For BHO and MIO, this shows the incremental changes due to the second stage. The benchmark is not dependent on the RO, however is given in relative terms for purpose of comparison. Only MG3 is chosen as it is the microgrid in which the FSO has the lowest runtime savings, and the largest variation in DER sizing. Solutions with objective function marked *infeas* are results that were infeasible and did not meet all of the demand (see ME).

Outage	Model	Rep. Days				Act. Days				
		runtime [s]	J [\$k]	PV [kW]	ESS [kWh]	runtime [s]	J [\$k]	PV [kW]	ESS [kWh]	
Grid connected	O1	RO	18.8	5140	11815	28409	19.4	6164	17148	55573
		BHO	+40.6	<i>infeas</i>	+0	+0	+40.9	<i>infeas</i>	+0	+0
		MIO	+63.8	+1570	+4967	+27770	+51.3	+546	+0	+56
		benchmark	+198.1	+1570	+4958	+27783	+197.4	+546	+0	+56
	O3	RO	15.1	5236	12385	31288	15.9	5324	12889	33860
		BHO	+40.6	<i>infeas</i>	+0	+0	+50.4	<i>infeas</i>	+0	+0
		MIO	+72.9	+470	+936	+1330	+55.5	+387	+12	+0
		benchmark	+109.8	+470	+965	+1298	+114.4	+382	+461	-1274
	O4	RO	16.4	4983	10796	23399	16.6	4558	7337	7923
		BHO	+46.4	+175	+0	+0	+46.3	+23	+0	+0
		MIO	+49.2	+175	+0	+0	+49.4	+23	+0	+0
		benchmark	+129.9	-551	-5086	-20371	+129.7	-127	-1628	-4904
Off-grid	O1	RO	13.5	4803	11815	28409	12.2	8683	17148	55573
		BHO	+41.8	<i>infeas</i>	+0	+0	+37.3	<i>infeas</i>	+0	+0
		MIO	+62.9	+6430	+30852	+48596	+62.3	+2550	+25696	+21259
		benchmark	+113.0	+6430	+30852	+48596	+115.6	+2550	+25696	+21259
	O3	RO	12.0	5215	12385	31288	12.0	5582	12889	33860
		BHO	+44.1	<i>infeas</i>	+0	+0	+43.9	<i>infeas</i>	+0	+0
		MIO	+62.7	+6018	+30270	+45719	+66.0	+5651	+29766	+43147
		benchmark	+133.9	+6018	+30270	+45719	+143.7	+5651	+29766	+43147
	O4	RO	11.3	4083	11803	28411	12.1	1823	7337	7932
		BHO	+53.2	<i>infeas</i>	+0	+0	+53.6	<i>infeas</i>	+0	+0
		MIO	+65.2	+7150	+31860	+53608	+64.2	+9410	+35318	+69075
		benchmark	+130.4	+7150	+31860	+53608	+130.1	+9410	+35318	+69075

by the results of the first model, to optimize only additional DER determined necessary. As part of the derivation of the model, we introduce a novel constraint on the state of charge of storage devices, which allows the representation of multiple day outages in the representative model, even though only a single representative day is optimized.

In future work we will include uncertainty in the input model to improve the correlation of the representative model with the optimal solution. Further, short-lived fluctuations that occur due to changes in demand and climate resource can have a significant impact on the Microgrid robustness when deployed in the field, but with hourly time-steps these fluctuations often average out. Therefore, we plan to extend the hybrid optimization framework to finer temporal resolutions, such as 15 or 5 minutes. Since the solution space increases exponentially with the number of time-steps, the run-time savings through HOs are potentially even more significant. Finally, we will analyze the impact of DER failure on the robustness of the solution.

Acknowledgements

The authors would like to acknowledge Adib Nasle and Scott Mitchell at XENDEE Inc. for their support in this work.

References

- [1] W. Ajaz, Resilience, environmental concern, or energy democracy? a panel data analysis of microgrid adoption in the united states, *Energy Research & Social Science* 49 (2019) 26–35.
- [2] N. Hatziargyriou, H. Asano, R. Iravani, C. Marnay, Microgrids, *IEEE power and energy magazine* 5 (2007) 78–94.
- [3] M. Stadler, A. Naslé, Planning and implementation of bankable microgrids, *The Electricity Journal* (2019).
- [4] Z. K. Pecanak, M. Stadler, K. Fahy, Efficient multi-year economic energy planning in microgrids, *Applied Energy* 255 (2019) 113771.
- [5] S. Mashayekh, M. Stadler, G. Cardoso, M. Heleno, A mixed integer linear programming approach for optimal der portfolio, sizing, and placement in multi-energy microgrids, *Applied Energy* 187 (2017) 154–168.
- [6] T. Schütz, M. H. Schraven, M. Fuchs, P. Remmen, D. Müller, Comparison of clustering algorithms for the selection of typical demand days for energy system synthesis, *Renewable energy* 129 (2018) 570–582.
- [7] Z. K. Pecanak, V. R. Disfani, M. J. Reno, J. Kleissl, Inversion reduction method for real and complex distribution feeder models, *IEEE Transactions on Power Systems* 34 (2018) 1161–1170.
- [8] G. Wu, W. Pedrycz, P. N. Suganthan, R. Mallipeddi, A variable reduction strategy for evolutionary algorithms handling equality constraints, *Applied Soft Computing* 37 (2015) 774–786.
- [9] H. Energy, Hybrid optimization of multiple energy resources, 2015.
- [10] D. Thevenard, G. Leng, S. Martel, The retscreen model for assessing potential pv projects, in: *Photovoltaic Specialists Conference, 2000. Conference Record of the Twenty-Eighth IEEE, IEEE, 2000*, pp. 1626–1629.
- [11] C. Marnay, G. Venkataramanan, M. Stadler, A. S. Siddiqui, R. Firestone, B. Chandran, Optimal technology selection and operation of commercial-building microgrids, *IEEE Transactions on Power Systems* 23 (2008) 975–982.
- [12] S. Chen, H. B. Gooi, M. Wang, Sizing of energy storage for microgrids, *IEEE Transactions on Smart Grid* 3 (2012) 142–151.
- [13] S. Bahramirad, W. Reder, A. Khodaei, Reliability-constrained optimal sizing of energy storage system in a microgrid, *IEEE Transactions on Smart Grid* 3 (2012) 2056–2062.
- [14] C. Milan, M. Stadler, G. Cardoso, S. Mashayekh, Modeling of non-linear chp efficiency curves in distributed energy systems, *Applied Energy* 148 (2015) 334–347.
- [15] Home - XENDEE microgrid platform, 2020. URL: <https://xendee.com/>.
- [16] T. Simpkins, D. Cutler, K. Anderson, D. Olis, E. Elgqvist, M. Callahan, A. Walker, Reopt: a platform for energy system integration and optimization, in: *ASME 2014 8th international conference on energy sustainability collocated with the ASME 2014 12th international conference on fuel cell science, engineering and technology, American Society of Mechanical Engineers, 2014*, pp. V002T03A006–V002T03A006.
- [17] K. Fahy, M. Stadler, Z. K. Pecanak, J. Kleissl, Input data reduction for microgrid sizing and energy cost modeling: Representative days and demand charges, *Journal of Renewable and Sustainable Energy* 11 (2019) 065301. doi:10.1063/1.5121319.
- [18] B. Bahl, A. Kümpel, H. Seele, M. Lampe, A. Bardow, Time-series aggregation for synthesis problems by bounding error in the objective function, *Energy* 135 (2017) 900–912.
- [19] P. Gabrielli, M. Gazzani, E. Martelli, M. Mazzotti, Optimal design of multi-energy systems with seasonal storage, *Applied Energy* 219 (2018) 408–424.
- [20] S. Pfenninger, Dealing with multiple decades of hourly wind and pv time series in energy models: A comparison of methods to reduce time resolution and the planning implications of inter-annual variability, *Applied energy* 197 (2017) 1–13.
- [21] M. Stadler, Z. K. Pecanak, P. Mathiesen, K. Fahy,

- J. Kleissl, Performance comparison between peak demand preserving day-type economic optimization and full time series approach for 13 US microgrids (submitted to *Applied Energy*, 2020).
- [22] P. Gabrielli, F. Fürer, G. Mavromatidis, M. Mazzotti, Robust and optimal design of multi-energy systems with seasonal storage through uncertainty analysis, *Applied energy* 238 (2019) 1192–1210.
- [23] M. Stadler, M. Groissböck, G. Cardoso, C. Marnay, Optimizing distributed energy resources and building retrofits with the strategic der-camodel, *Applied Energy* 132 (2014) 557–567.
- [24] T. Schittekatte, M. Stadler, G. Cardoso, S. Mashayekh, N. Sankar, The impact of short-term stochastic variability in solar irradiance on optimal microgrid design, *IEEE Transactions on Smart Grid* 9 (2018) 1647–1656.
- [25] M. Stadler, Effect of heat and electricity storage and reliability on microgrid viability: a study of commercial buildings in california and new york states (2009).
- [26] S. Mashayekh, M. Stadler, G. Cardoso, M. Heleno, S. C. Madathil, H. Nagarajan, R. Bent, M. Mueller-Stoffels, X. Lu, J. Wang, Security-constrained design of isolated multi-energy microgrids, *IEEE Transactions on Power Systems* 33 (2017) 2452–2462.